2022 IEEE 22nd Annual Wireless and Microwave Technology Conference (WAMICON) | 978-1-6654-2195-9/22/$31.00 ©2022 IEEE | DOI: 10.1109/WAMICON53991.2022.9786160

Advanced Manufacturing of Passive Wireless High-Temperature Pressure Sensor Using 3-D Laser Machining

Seng Loong Yu[1], Swadipta Roy[2], Sreekala Suseela[2], Taofeek Orekan[2], Joshua McConkey[2], Reamonn Soto[2], Eduardo A. Rojas-Nastrucci[1]
[1]*Department of Electrical Engineering and Computer Science*
Embry-Riddle Aeronautical University
Daytona Beach, USA
[2]*Sensatek Propulsion Technology, Inc.*
Daytona Beach, USA
yus5@my.erau.edu, {sroy, spapali, torekan, josh, rsoto}@sensatek.com, rojase1@erau.edu

***Abstract*—Recent radio-frequency resonance-based high-temperature sensors have enable the next generation of passive wireless sensing for harsh environments, such as inside of jet engines. A novel manufacturing technique for an evanescent-mode-resonator-based and antenna-integrated wireless passive pressure sensor is proposed therein. This technique employs a planar PCB manufacturing tool to laser etch a 3-D structure on an alumina substrate. A laser machining study is conducted to find etch consistency and fine-tune laser etching parameters. The wireless passive pressure sensor is tested through various mechanical and thermal loads to measure its performance. The sensor is proven to work in the range of 25 °C–1700 °C, sensing pressures of 0 psi to 163 psi with resonances within the frequency range of 6.33 GHz–6.7 GHz.**

***Index Terms*—Wireless, RF, high temperature, pressure sensor, manufacturing, laser machining.**

I. Introduction

Recent discoveries on harsh-environment RF-based sensing mechanisms have triggered a new set of wireless sensing technologies being developed to sense in environments that traditionally were out of reach, such as the interior of a gas turbine. Pressure monitoring is an essential part of gas turbine engine operation. Optimal pressure ratio is required to maximize thermal efficiency in turbine engines. Efficient gas turbines may have internal temperatures up to 1600 °C [1]. Furthermore, real-time monitoring of pressure inside the gas turbine is also necessary for safe operation. Therefore, it is desired to have a wireless passive sensor with robust characteristics that could withstand the harsh environments of the gas turbine engine.

Wireless sensing techniques have been shown over the years with integrated active/passive devices [2], MEMS-based capacitive-loaded [3], and even SAW-based sensors [4]. While being able to achieve robust performance in Q factor and sensitivity, these approaches may not survive in conditions up to 1600 °C. On the other hand, resonator/antenna integration on ceramics-based materials [5] has shown to provide robust performance up to 1000 °C. In [6], an low-profile wireless passive temperature sensor using resonator/antenna integration is shown to perform up to 1000 °C. Finally, an evanescent-mode-resonator based passive wireless sensor is integrated with a patch antenna [7] is able to detect changes in pressure while also being able to survive up to temperatures of 800 °C.

In this work, a novel manufacturing technique is developed to fabricate a pressure sensor based on evanescent-mode resonance as described in [7]. The fabrication of the pressure sensor described in [7] employs a Teflon mold that is first micromachined and the deposition of the liquid ceramic material. To solidify the final sensor, UV curing and sintering steps are required in the final stages of fabrication. The novelty of the laser-based manufacturing in this paper is that the same sensor cavity geometry is achieved by the use of a planar PCB manufacturing tool, the LPKF ProtoLaser system, to fabricate 3-D structures using its laser capabilities. This is done by etching or burning material off the substrate with very fine tune laser settings to create the desired structure — this manufacturing process is also known as subtractive manufacturing. This manufacturing technique provides an alternative low-cost, low-infrastructure, and low-time solution. To optimize the fabrication process, a laser etch rate experiment and study was conducted to find the number of repetitions required to create certain depths on the chosen substrate. The manufactured wireless sensor is then tested and its performance is measured up to the temperature requirements of 1700 °C using methods described in [8]. Measurements indicate that the manufactured sensor may operate from 25 °C to 1700 °C, sensing pressures from 0 psi to 163 psi with resonant responses varying from 6.33 GHz to 6.7 GHz.

II. Material Selection, Simulation and Design

In [7], a polymer-derived ceramic (PDC) was used to develop the sensor for temperatures up to 800 °C. To accommodate for even higher temperature environments such as a turbine engine, which may rise up to 1700 °C, alumina (Al_2O_3) is selected as the material for the pressure sensor.

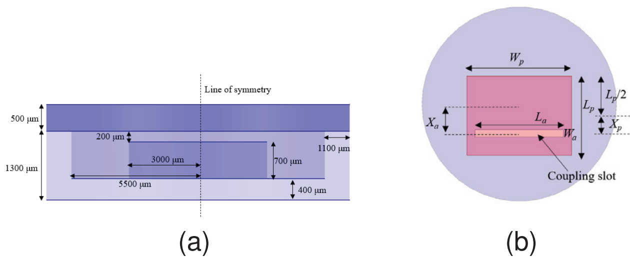

Fig. 1. Dimensions of (a) sensor cavity and (b) integrated antenna.

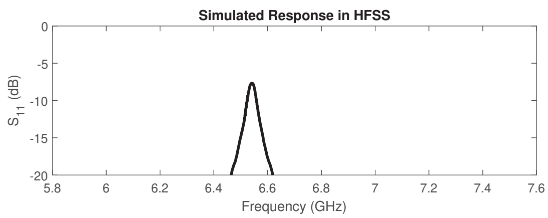

Fig. 2. Simulated response (TD-gated) of S_{11} when sensor is interrogated by antenna.

Alumina is a well-known material to survive in such harsh environments, especially since commercial alumina can be easily purchased with relatively high purity. Furthermore, alumina has been used previously to be cut with high-precision laser machining systems, such as the LPKF ProtoLaser which is also used in this study.

The sensor geometry from [7] is studied and used in this work, with cavity resonator dimensions as indicated in Fig. 1a and integrated antenna with dimensions $W_a = 7.1$ mm, $L_p = 5.4$ mm, $W_a = 0.5$ mm, $L_a = 6$ mm, $X_a = 2$ mm, and $X_p = 0.8$ mm, as shown in Fig. 1b. Due to differences in material properties, the expected resonant frequency using alumina will shift downward, as indicated in [6]. It is important to note that the interrogating antenna must be designed separately to accommodate the expected lower resonant frequency. In this paper, a custom-designed Vivaldi antenna is used to interrogate the wireless passive sensor. The design of both the pressure sensor and interrogation antenna were both simulated in Ansys HFSS. Time-domain (TD) gating is applied to the to S-parameters isolate responses from just the sensor itself [6]. The TD-gated reflection coefficient (S_{11}) indicates that the resonance occurs around 6.54 GHz, as shown in Fig. 2.

III. Manufacturing of Wireless High-Temperature Pressure Sensor

A. Laser Etch Rate Study on Alumina Substrate

The LPKF ProtoLaser system is used to etch material off an alumina substrate to achieve the desired structure. Traditionally, this PCB manufacturing system is typically used for creating planar circuits in rapid prototyping environments. Since the system is equipped with an ultraviolet laser with an operating wavelength of 355 nm and a maximum output power of 5.7 W, experiments were conducted with various parameters to find etching consistency. From the experiments, consistent material etching is achieved by setting the output power to its maximum (5.7 W) and a repetition rate of 45 kHz. Furthermore, the spacing between each route is set to 10 μm for both consistency and production speed. It was found through the experiments that the default spacing of 20 μm leads with rough surfaces between the routes thus reducing the spacing to 10 μm mitigates this surface roughness issue.

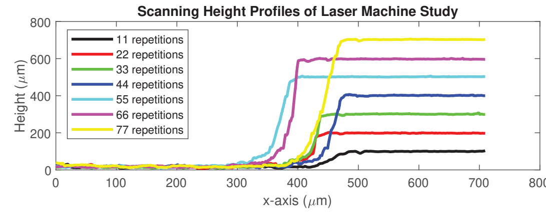

Fig. 3. Height profiles of etched circle array of various repetitions rates.

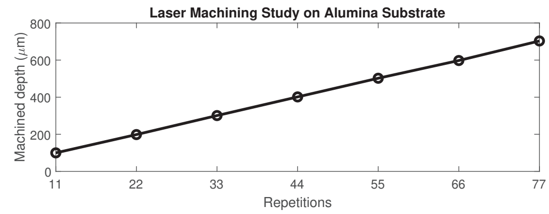

Fig. 4. Summary of machined depths versus number of repetitions.

Next, a study of laser etch rate is conducted. This information is needed to manufacture the final sensor, whose geometry consists of a post, a cavity, and the outline. With the aforementioned laser parameters of 5.7 W peak power, repetition rate of 45 kHz, and spacing of 10 μm, a repetition versus depth study and conducted. It was found overall that the etch rate is approximately linear with material being etched off at 100 μm per 11 repetitions. This is equal to an etch rate of 9.1 μm/repetition. In Fig. 3, trenches with diameter of 2 mm are generated at repetitions of 11, 22, 33, 44, 55, 66, and 77. The resulting mean trench depths are 99.79 μm, 198.42 μm, 300.92 μm, 401.52 μm, 502.16 μm, 597.69 μm, and 703.23 μm respectively. Fig. 4 shows the etch rate profile plot, agreeing with an etch rate of approximately 9.1 μm/repetition.

B. Final Manufacturing Parameters of Pressure Sensor

The final manufacturing process of the pressure can be encapsulated into three sections: post (inner circle), cavity, and outline cutting of sensor. A 1.3 mm alumina sheet is used as the substrate to achieve the desired wall height. To ensure alignment during the fabrication process, the whole fabrication process must be done sequentially without removal of the alumina substrate from the machining chamber.

Furthermore, the post and cavity are both material etching processes. Therefore, the laser etch study in the previous may be used to create these structures. For both the post and cavity, the output power is set to 5.7 W with a repetition rate of 45 kHz. Since the post and cavity have depths of 0.2 mm and 0.9 mm respectively, referring to Fig. 4 a repetition of 22

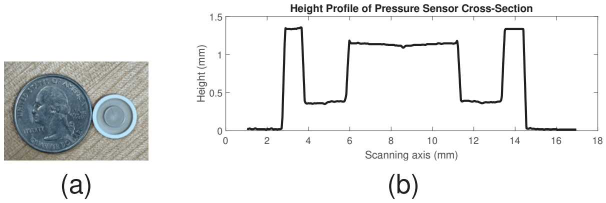

Fig. 5. (a) Sensor cavity versus a quarter for size comparison and (b) cross-section height profile of manufactured sensor.

and 99 were used to machine these geometrical structures. Finally, the final section – the outline cutting of the sensor is processed. To ensure that the pressure sensor is fully cut out, the default profile used for general cutting is sufficient with a total repetition of 600 passes.

The fabricated sample is shown in Fig. 5a. A cross-section line scan was also done to obtain the numerical height which can then be extracted and plotted as shown in Fig. 5b. As shown, height profiles of the post, cavity, and outer wall were found to be 1.1 mm, 0.4 mm, and 1.3 mm respectively, agreeing with the design values that was described in original paper [7].

The integrated antenna is then manufactured by first cutting out an alumina cap and accompanying solder masks with the LPKF ProtoLaser system. Applied Technologies 8667-F platinum ink is then applied on the solder mask to create the conductive traces. After curing, the caps with conductive traces is then fired to sinter the platinum particles. Finally, the cap is binded to the manufactured cavity with MTI EQ-CAA-2-LD alumina adhesive.

IV. RESULTS

In this section, the pressure sensor is tested over different pressures at moderately high temperature to demonstrate its working mechanism. The test setup shown in Fig. 6 is used in order to apply simultaneously both thermal and mechanical loads, while using a wireless antenna. The pressure sensor is put inside the heat pad, which also provides a rigid backing surface to the sensor while under mechanical loads (pressure). The heat pad is used to control the temperature of the sensor, while a type-K thermocouple provides a second temperature reading of the heat pad chamber. A Dillon 36321-0030 GL force gauge is used to apply and control the mechanical load exerted on the sensor through an alumina rod. Fiberfrax blanket is used to cover the heat pad to stabilize the temperature of the pressure sensor. A Vivaldi antenna kept right above the Fiberfrax blanket on top of the pressure sensor is used to read wirelessly the resonant signal from the sensor, when it is under simultaneous mechanical and thermal loads. The Vivaldi antenna allows the wireless interrogation of the sensor without the need of being directly on top of the sensor and is connected to a Copper Mountain Technologies R140 vector network analyzer (VNA) to measure the response of the pressure sensor.

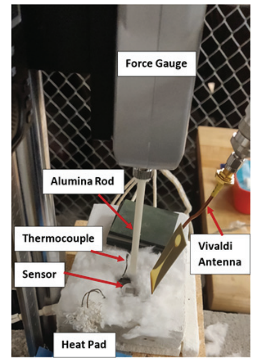

Fig. 6. Measurement setup for testing of pressure sensor.

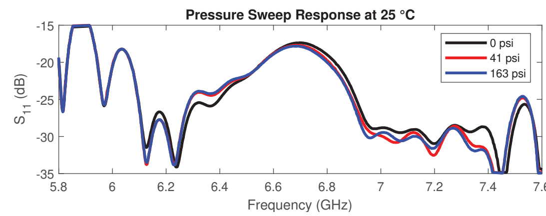

Fig. 7. Pressure sensor readings (frequency vs amplitude) at a variety of pressures at 25 °C.

Using this setup, tests were performed at different pressures up to 163 psi and temperatures up to 703 °C. The resonant signals of the sensor at room temperature (25 °C) with no mechanical load and at 703 °C with a pressure of 163 psi are shown in Fig. 7 and Fig. 8. The resonant peak was clearly distinguishable from the noise background and we can see a clear shift of the resonant frequency from 6.697 GHz to 6.329 GHz due to the combined effect of pressure and temperature.

At room temperature, the resonance frequency started decreasing slowly as the pressure is increased. Fig. 7 shows the sensor's response at 0 psi, 41 psi and 163 psi while the temperature of the sensor was kept at 25 °C. The resonant peak remained distinguishable with a high signal to noise ratio even up to 163 psi, which is very good.

At higher temperatures with no pressure (0 psi), the resonance decreased as the temperature is increased. While the resonant peak is still distinguishable, the signal to noise ratio began to degrade at 201 °C. Fig. 8 shows the sensor's response at 100 °C, 201 °C, 402 °C, and 703 °C with no pressure applied. At 703 °C, the resonance frequency still decreased as the pressure is increased. Fig. 9 shows the sensor's response at 0 psi, 90 psi and 163 psi while the temperature of the sensor was kept at 703 °C. The resonant peak remained distinguishable even with the background noise, which is very good. This shows that the sensor could still clearly detect different pressures at such high temperature.

Fig. 10 shows the overall response of the sensor at different pressures up to 163 psi and various temperatures up to 703 °C. At each of the temperatures examined, the resonant frequency decreased quasi-linearly when the pressure is increased due to the reduction of the gap inside the sensor. This proves

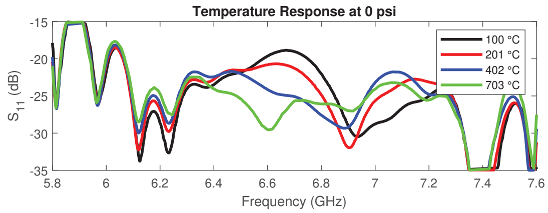

Fig. 8. Pressure sensor readings (frequency vs amplitude) at a variety of temperatures with 0 psi.

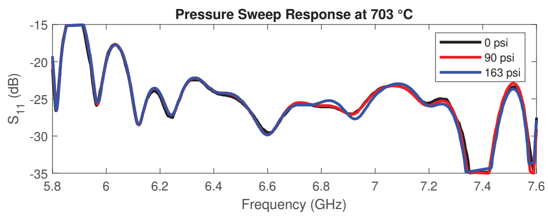

Fig. 9. Pressure sensor readings (frequency vs amplitude) at a variety of pressures at 703 °C.

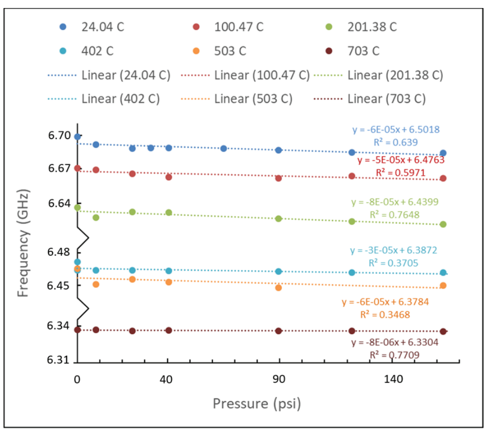

Fig. 10. Change in resonant frequency of the pressure sensor with applied pressure at various temperatures.

the working mechanism of the pressure sensor at a wide range of pressures in various temperature environment. This is an important milestone for wireless pressure sensor in high temperature environment.

Finally, the sensor was also put through a ramp of temperature up to 1700 °C. Shown in Fig. 11, the frequency response after the temperature ramp shows the resonant frequency shift to a lower value. Other than that, the magnitude of the resonant frequency peak is also significantly deteriorated by about 10 dB or so. This phenomenon can be explained when the time domain response is acquired. When transformed to the time domain, there seems to be excessive ringing within the first 20 ns. This ringing will cause energy contained within the cavity to be dissipated over time, due to low amplitude resonance. Other than that, it is also hypothesized that the testing environment in a furnace with heating coils would also cause some RF interference.

In a real pressure-monitoring system, very small frequency

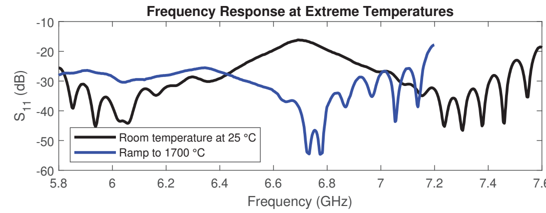

Fig. 11. Frequency response at room temperature and at 1700 °C.

differences can be determined by using very high density of points in the frequency domain. Further, differential analysis using a real pressure sensor and one whose diaphragm has a small hole (equalizing its pressure) can be placed in proximity. Both will change equally in resonant frequency with temperature, and the difference in frequency between the two will be the pressure signal.

V. Conclusion

In this paper, the design, simulation, and of a wireless passive sensor is described. The design of the sensor and interrogating antenna is first simulated in HFSS indicating resonance at 6.54 GHz. A laser machine study is subsequently conducted to find etching rates for alumina. The wireless sensor is then manufactured using information from the study. Finally, the wireless was tested at various temperatures and pressures, verifying its operation at 25 °C–1700 °C and at 0 psi–163 psi.

Acknowledgment

The authors would like to express gratitude to Embry-Riddle Aeronautical University for the financial support of this publication. This work is supported by the National Science Foundation under Grant 1944599 and the Department of Energy under Contract DESC0020800.

References

[1] MHI Group, "MHI Achieves 1,600°C Turbine Inlet Temperature in Test Operation of World's Highest Thermal Efficiency 'J-Series' Gas Turbine." MHI.com. https://www.mhi.com/news/1105261435.html (accessed Jan. 31, 2022).

[2] M. C. Scardelletti, J. L. Jordan, G. E. Ponchak and C. A. Zorman, "Wireless capacitive pressure sensor with directional RF chip antenna for high temperature environments," 2015 IEEE International Conference on Wireless for Space and Extreme Environments (WiSEE), 2015, pp. 1-6.

[3] S. Scott and D. Peroulis, "A capacitively-loaded MEMS Slot element for wireless temperature sensing of up to 300°C," 2009 IEEE MTT-S International Microwave Symposium Digest, 2009, pp. 1161-1164.

[4] G. Bruckner, J. Bardong, P. Szász and S. Oschkera, "Wireless, direct pressure sensing with saw devices at elevated temperatures," 2018 IEEE International Ultrasonics Symposium (IUS), 2018, pp. 1-9.

[5] X. Gong and L. An, "Low-profile wireless passive resonators for sensing," U.S. Patent 9612164B2, Apr. 4, 2017.

[6] H. Cheng, S. Ebadi and X. Gong, "A Low-Profile Wireless Passive Temperature Sensor Using Resonator/Antenna Integration Up to 1000 °C," in IEEE Antennas and Wireless Propagation Letters, vol. 11, pp. 369-372, 2012,.

[7] H. Cheng et al., "Evanescent-mode-resonator-based and antenna-integrated wireless passive pressure sensors for harsh-environment applications," Sens. Actuators A, Phys., vol. 220, pp. 22–33, Dec. 2014.

[8] R. Soto, "Apparatus, systems, and methods for wireless monitoring of gas turbine engine temperature," WIPO (PCT) Patent WO2019100082A1, May 24, 2019.